Radial and Axial Integrated Auxiliary Bearing Device for Active Magnetic Bearing System

Wei SONG[a], Chengtao YU[a], Yuemei SUN[a], Xiuxiang CHEN[a]

[a] Jiangsu University of Technology, 1801 Zhongwu Rd., Changzhou, China, yuct@jsut.edu.cn

***Abstract*—A type of radial and axial integrated auxiliary bearing (RAIAB) device with the function of simultaneously eliminate the radial and axial protective clearance after the magnetic levitated rotor dropped is conceived and presented in this paper. In the RAIAB, the two ends of the rotor and the inner races of the RAIABs mounted in each end are machined into cone-shape coordination. Besides, a series of ball are used between the outer races of the RAIABs and the pedestal. When the active magnetic bearing works, initial protective clearances exist between the two ends of the rotor and the inner races. After AMB system failure, the auxiliary bearing driven by an additional motor to produce axial movement which makes the cone surfaces of the inner races of auxiliary bearings gradually close with each end of the rotor until the protective clearance is eliminated. Therefore, the possibility of backward whirl and impacts can be reduced. Two different cone schemes of the rotor end shape are comparatively diskussed. Furthermore, the influences the value of taper of the cone on the protective clearance between the rotor and auxiliary bearing and the axial force produced by the radial force after the rotor drop. The preliminary prototype experimental rig was developed to demonstrate the feasibility of the RAIAB.**

I. INTRODUCTION[1]

Active magnetic bearing (AMB) systems have many unique advantages over the conventional rolling element bearing and oil-film bearings, such as rotor vibration controllable, noise reduction and high D_n value. Since no metal-metal contact occurs in system, issues of wear, lubrication and limited life can be avoided. Therefore, AMB is well suited to the needs of some special applications, such as high speed, high precision, small volume, vacuum and so on[1-2]. Nevertheless, the AMB-suspended rotor requires an auxiliary bearing system to ensure the safety of AMB system and to support continuous and reliable operation even at AMB system power-down.

Most conventional auxiliary bearing designs use rolling element bearings. Usually, a fixed protective clearance whose length is approximately one-half of the AMB air gap is existed between the inner race of the bearing and the rotor. However, due to this fixed clearance, large dynamic forces will be generated after the high rotating speed rotor drops, even the rotor might susceptibly induce backward whirl. And those large dynamic forces are the main reason of auxiliary bearings damages and even more serious the AMB rotor and stator may be destroyed[4-8]. Therefore, some other types of auxiliary bearings have been developed. A type of Zero Clearance Auxiliary Bearing (ZCAB) was presented by Mohawk Innovative Technology, Inc. (MiTi)[9-10]. In the ZCAB, a series of small ball bearing are mounted surround the rotor. After the rotor drops, those ball bearings could move circumferentially and radially inward to eliminate the protective clearance between the rotor and ZCAB. The disadvantage of ZCAB the rotating speed of those ball bearings would be several folds more than that of the rotor, and that speed may exceed the limited speed of those ball bearings. Besides, an air foil bearing was suggested to integrate into the AMB system as auxiliary bearing[11-12]. However, both its mechanical structure and control system are complicated. WU et al. designed a device with an electromagnet as auxiliary bearing[13]. This device could eliminate the clearance between the rotor and itself by releasing the device under power-down conditions. But, apart from power-down, it couldn't work properly in other conditions. In this paper, a type of radial and axial integrated auxiliary bearing (RAIAB) device which can eliminate the radial and axial protective clearance simultaneously is presented. Firstly, the structure and operating mechanism of RAIAB are introduced. Following that, two different cone schemes of the rotor end shape are comparatively discussed. Furthermore, the influences the value of taper of the cone on the protective clearance between the rotor and auxiliary bearing and the axial force produced by the radial force after the rotor drop. Finally, the performances of an RAIAB are experimentally analyzed.

II. RAIAB STRUCTURE AND OPERATING MECHANISM

Figure 1 shows a schematic diagram of the structure of a radial and axial integrated auxiliary bearing. The auxiliary bearing is composed of an inner bush, a rolling bearing, a screw-in disk, balls, a base and an end cap. The rotor end and inner surface of the inner bushing are machined into conical surfaces, so that the radial clearance L_r and axial clearance L_a exist between these two conical surfaces simultaneously. The inner ring of a pair of angular contact ball bearings is installed with an inner bushing, and the outer ring is pressed axially by the end cover and the screw-in disk. The screw-in disk and the base are supported by a number of ball bearings uniformly distributed along the circumferential direction. The outer surface of the joint between the end cap and the base is symmetrically provided with a plurality of spiral grooves (similar to multiple-thread) symmetrically along the circumferential direction. The displacement of the groove along the axial direction is greater than $2L_a$. The base and the body are fixedly connected, and corresponding parts of the inner surface of the base are left with two protrusions with a

[1] National Nature Science Foundation of China (51605208); Natural Science Foundation of the Jiangsu Higher Education Institutions of China (Grant No.16KJB460008); Major project of natural science research in universities of Jiangsu (Grant No.16KJA460002)

certain circumferential width, which can be matched with the grooves of the end caps. In addition, the outer surface of one end of the screw-in disk away from the rolling bearing is machined with a gear and connected to a additional stepping motor. The principle of elimination of the gap in the radial and axial integrated auxiliary bearing is that when the magnetic bearing works normally, the relative position angle between the screw-in disk and the base is adjusted, so that there are normal radial clearance and axial clearance between the inner bushing and the rotor end conical surface. When the rotor is dropped, the additional motor drives the screw-in disks and the end cover to rotate relative to the base. Because of the spiral groove in the end cover, the rotation of the screw-in disk relative to the base is transformed into a linear movement of the screw-in disk along the axial direction. Therefore, the rolling bearing and the inner bushing are driven to move axially close to the rotor, and at the same time, the radial and axial clearances between the rotor and the inner bushing are eliminated.

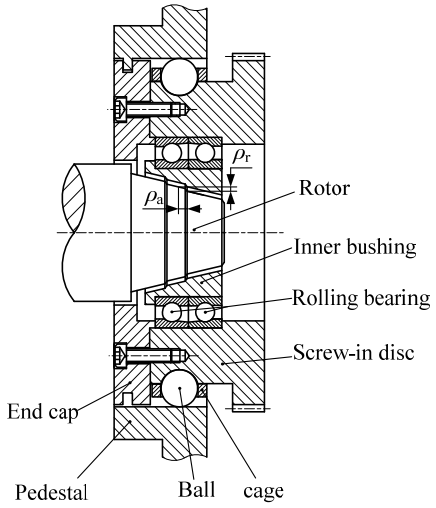

(a) Normal working state of magnetic bearing

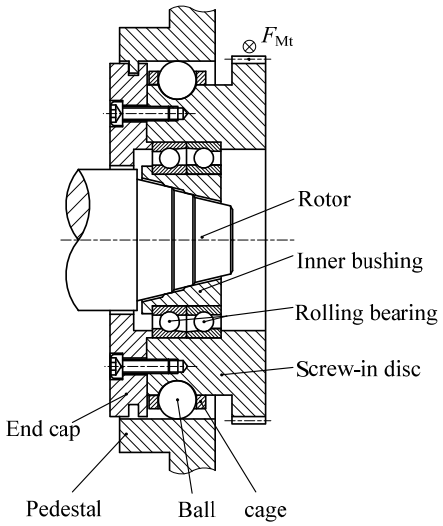

(b) The state of auxiliary bearing eliminate clearance

Figure 1. Radial and Axial Integrated Auxiliary Bearing Device Concept Sketch

III. INFLUENCES OF SHAPES OF ROTOR ON PROTECTIVE CLEARANCE

As shown in Figure 2(a), a schematic diagram of the protective clearance between the rotor and the inner bushing is shown. When the taper of the rotor end is θ_1, the clearance between the radial direction and the axial direction of the rotor are ρ_r and ρ_a, respectively. However, due to the characteristics of the cone, the closest point of point A on the cone surface of the rotor and the inner bush is point A', and the distance between them is as follows:

$$AA' = \rho_r \cos\theta_1 \tag{1}$$

When the rotor moves along the direction of the AA', the actual radial and axial protective clearances between the rotor and the inner bushing will be less than ρ_r and ρ_a.

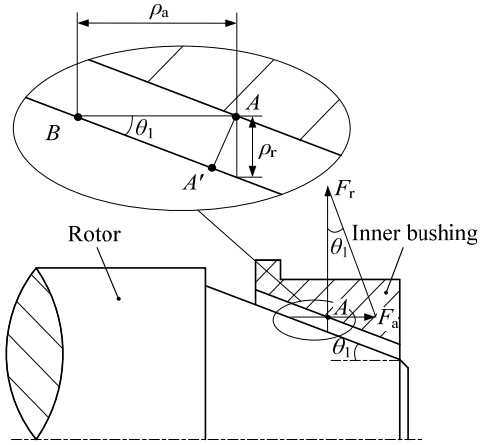

(a) the state of force and clearance between the rotor end and the inner bushing with only one taper

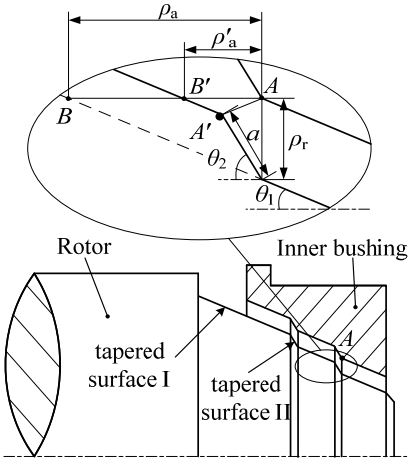

(b) the state of clearance between the rotor end and the inner bushing with two tapers

Figure 2. Comparisons of Two Shapes of Rotor End and Inner Bushing

In addition, when the rotor radial clearance is set to ρ_r, the relationship between the axial clearance ρ_a and the radial clearance ρ_r is:

$$\rho_a = \rho_r / \mathrm{tg}\theta_1 \tag{2}$$

That is, the axial protective clearance is affected by the taper of the rotor, and the relationship between axial protective clearance and rotor taper is shown in Figure 2(a). It can be seen from the figure that when the taper is θ_1=45°, ρ_a and ρ_r are equal; when θ_1<45°, ρ_a is greater than ρ_r; and when θ_1>45°, ρ_a is smaller than ρ_r. The relationship between the actual clearance and the rotor taper is shown in Figure 2(b). It is shown that the actual clearance will be smaller than the radial clearance ρ_r, and decreases with the increase of rotor taper. When the taper is θ_1=45°, the actual clearance AA' between the rotor and the inner bushing is only $0.72\rho_r$.

When the rotor with the taper θ_1 is in contact with the inner bushing, the axial impact force F_a will be generated simultaneously with the radial collision force F_r:

$$F_a = F_r \mathrm{tg}\theta_1 \tag{3}$$

It can be obtained that the axial impact force F_a will increase sharply with the increase of θ_1, as the axial force F_a hinders the elimination of the mechanism clearance, a sharp increase in F_a will be detrimental to the performance of the mechanism.

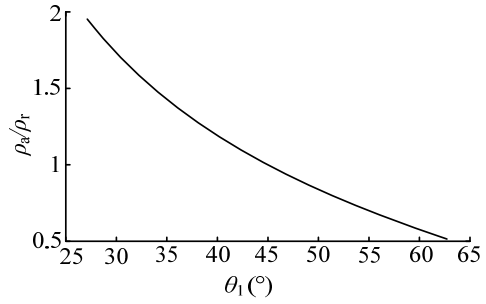

(a) The relationship between ρ_a/ρ_r and θ_1

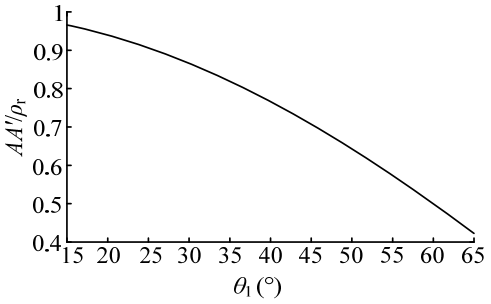

(b) The relationship between AA'/ρ_r and θ_1

Figure 3. Influence of the taper of the cone of rotor end on protective clearance

As shown in Figure 2(b), the rotor ends are alternately composed of two types of cones. Among them, the taper θ_1<θ_2, so that after the clearance is eliminated, the rotor and the inner sleeve contact with the taper at the taper of θ_1 Since the taper is small, no large axial force is generated; at the same time, the taper θ_2 shortens the rotor and axial clearance between inner bushing ρ'_a

$$\rho_a^{'} = \rho_r / \mathrm{tg}\theta_1 - a\sin(\theta_2 - \theta_1)/\sin\theta_1 \tag{4}$$

Where, a is the length of the cone with taper θ_2. Let a=$\kappa\rho_r$ then the Eq. (4) is changed to:

$$\rho_a^{'} = \frac{\cos\theta_1 - \kappa\sin(\theta_2 - \theta_1)}{\sin\theta_1}\rho_r \tag{5}$$

However, the actual clearance AA' is changed to:

$$AA' = \rho_r\sqrt{\kappa^2 - 2\kappa\sin\theta_2 + 1} \tag{6}$$

For magnetic bearings, the axial protective clearance is generally close to the radial protective clearance. Make $\rho_a^{'} = \rho_r$ in the Eq. (5) get that when this requirement is met, the value of taper and the length of the Cone II are shown in Figure 4(a). It can be seen that when the taper θ_1 of cone I is certain, the taper θ_2 of Cone II is inversely proportional to its length a. That is to say, the length a of Cone II is small, it requires a larger taper θ_2 to satisfy the condition $\rho_a^{'} = \rho_r$. And with the reduction of taper θ_1 the taper θ_2 needed increases in the case that the length a of the same cone I is unchangeable. Figure 4(b) is the actual clearance AA' between the rotor and the neck bush calculated by application Eq. (6), in the case of the corresponding κ and θ_2 in Figure 4(a). Figure 4(b) show that when the condition $\rho_a^{'} = \rho_r$ is satisfied, AA' are always smaller than ρ_r. Furthermore, AA' is first reduced and then increased with the increase of a and AA' decreases with decrease of the θ_1.

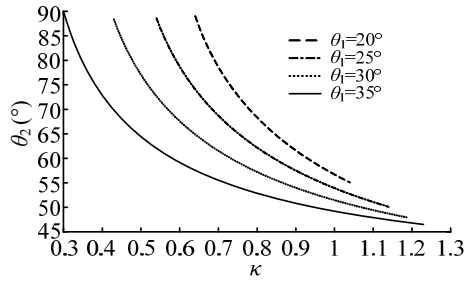

(a) Values of θ_2 and K at the condition of ρ_a=ρ_r

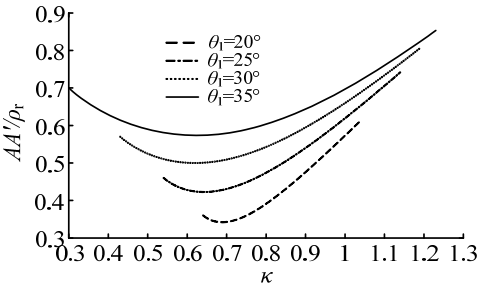

(b) Values of AA'/ρ_r at the condition of ρ_a=ρ_r

Figure 4. Values of each parameter under the rotor with two types of cones.

By comparing the Figure 3 with Figure 4, it could be found that when the rotor and the inner bushing consist of only one kind of taper, the taper of the cone θ_1 equals to 45° when ρ_a=ρ_r. While, the actual clearance AA' between the rotor and the inner bushing is changed to $0.72\rho_r$ and the axial force F_a produced by the radial force equals to F_r. When the cones of the rotor ends and the inner bushing adopt two kinds of taper, under the same conditions that ρ_a=ρ_r and AA'=$0.72\rho_r$, the

minimum value of θ_1 can be reduced to 25°, and the produced axial force after the clearance is eliminated can be reduced to F_a=0.47F_r.

IV. RAIAB Tests and Results

A. Test Setup

Figure 5 shows a diagram of the structure of a magnetic bearing with active and passive integrated auxiliary bearings. The two ends of the rotor of the magnetic bearing are modified to install the active and passive integrated auxiliary bearings and additional motors shown in Figure 2. Moreover, the control system of the additional motors is integrated with the electronic control system of the AMB.

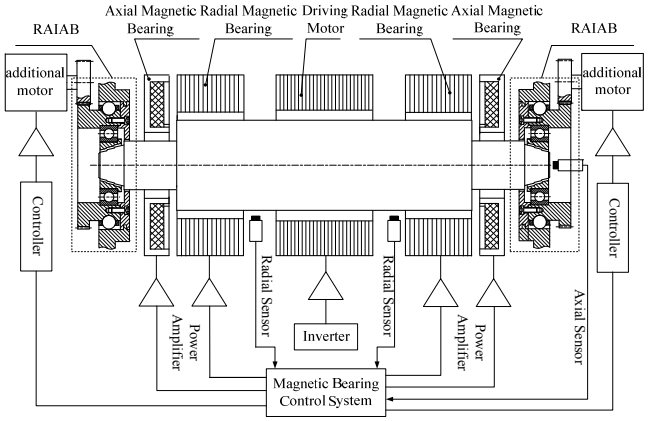

Figure 5. Schematic of RAIAB Test Rig

Figure 6 shows the picture of the test rig. The rotor weight of the test bench rotor is 2.4 kg and the length is 350 mm. It is completely suspended by an AMB system, and by a motor to provide the rotary drive force to the rotor. By cutting off the whole power supply of the magnetic bearing system, the radial and axial drop of the rotor can be achieved by 5 degrees of freedom. The speed of the rotor and inner bushing is detected by an optical fiber sensor. The displacement signal of rotor radial and bearing is collected by data acquisition card. The speed of the motor is regulated by the inverter. Additional motor controlled by additional motor controller. The current of the magnetic bearing is monitored in real time. After the magnetic bearing switch is turned off, the current sensor detects that the current is reduced to zero, and sends the signal to the additional motor controller immediately to make the additional motor work immediately, and the additional motor drives the inner bushing to rotate through the gear drive. In order to verify the performance of RAIAB, the taper of the inner bushing and the rotor was initially chosen to be 30°. The radial protective clearance between the rotor and the inner bushing is 0.15 mm and the axial protective clearance is 0.25 mm.

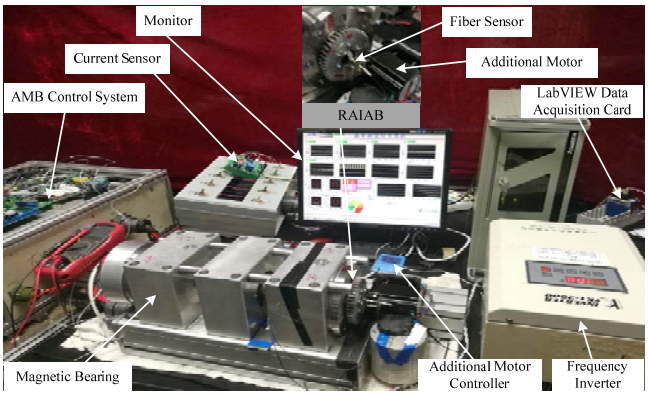

Figure 6. Experimental Facility

B. Tests Results

The rotor orbits of the left and right ends of the rotor within 1.6 s after dropping to RAIAB at speed 6,000 rpm are shown in Figures 7(a) and 7(b). The directions of the X and Y axis coincide with the magnetic pole direction of the AMB and are obtained by rotating the horizontal and vertical directions 45° along the counterclockwise, It can be seen from the result shown in figure 7 that the rotor is pushed back to the position near the center after several impacts.

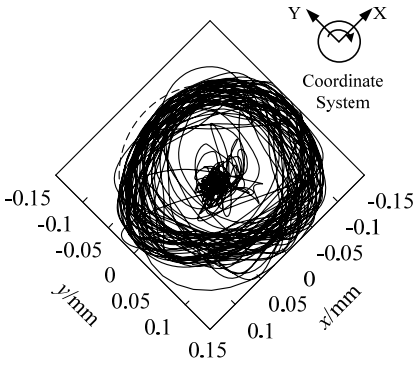

(a) Left side of rotor

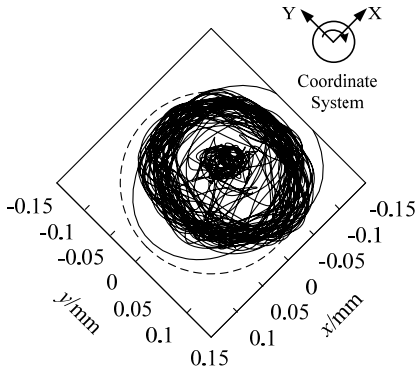

(b) Right side of rotor

Figure 7. Orbits of rotor's center

Figures 8 (a) and (b) show the detailed X and Y displacements of the left and right ends of the rotor. Fig. 9 shows the vibration displacement of the Z direction of the rotor.It can be seen from Fig. 8 that the rotor dropped at about

0.1 s, and after the fall, the rotor and RAIAB collided violently. At nearly 0.8 s, the vibration displacement decreased significantly until about 0.9 s ,and it entered a stable periodical small vibration;When entering a stable vibration, the vibration displacement of the left and right ends of the rotor in each direction is a maximum of about 30 μm. From the result of the axial displacement shown in Fig.9, the axial displacement of the rotor after dropping at about 0.1 s can reach nearly 0.4 mm, and then the vibration amplitude slightly decreases until it is about 0.08mm after about 0.9 s. The position is stable and the vibration displacement is only 1.4 μm. Since the additional motor drive scheme used in this paper is to start to provide the controller signal when the current sensor detects the current in the magnetic bearing is less than 0.1 A, thereby controlling the rotation of the motor. When the magnetic bearing current is less than 0.1 A, the controller immediately drives the additional motor to rotate thescrew-in disk. At this time, the clearance is gradually eliminated. After the clearance is completely eliminated, the rotor is stably supported by the RAIAB.

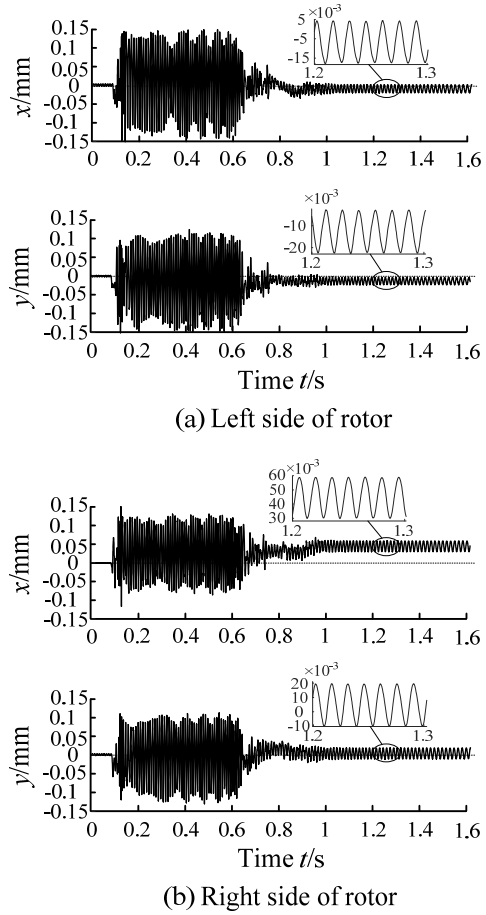

Figure 8. Figure 8. Radial displacement of the dropping rotor at 6,000 rpm

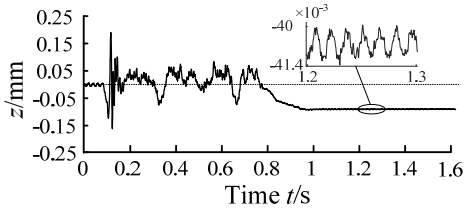

Figure 9. Axial displacement of the dropping rotor at 6,000 rpm

Figure 10 shows the displacement of the left end of the rotor in the X direction at different speeds. It can be seen from the figure that the clearance elimination time after the rotor is dropping is basically the same, which is about 1 s. With the increase of rotational speed, the vibration displacement when the rotor is stably supported by the RAIAB slightly increases. For example, when the rotation speed is below 15,000 rpm, the vibration displacement is about 30 μm. At 21,000 rpm, the vibration displacement increased to 40 μm, which may be due to the fact that the centrifugal force of the rotor increased with increasing speed.

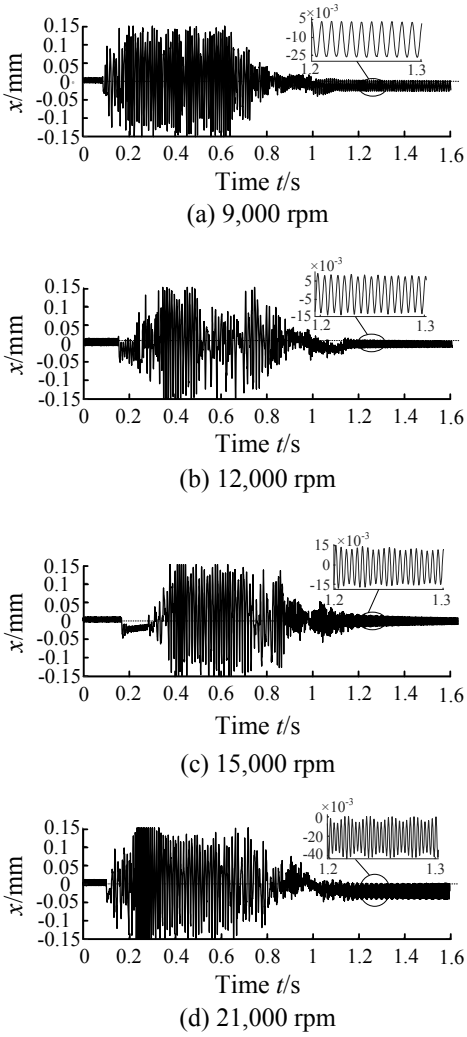

Figure 10. Displacement of the left end of the rotor in the X direction at different rotational speeds

Figure 11 shows the vibration displacement of the rotor in the Z direction at different speeds.As can be seen from the figure, the Z direction of the rotor is basically stable within 2 μm after the rotor has dropped for approximately 1 s.Comparing the X- and Z-direction vibration displacements at each rotation speed in Fig. 10 and Fig. 11, it can be seen that due to the centrifugal force of the rotor radial direction, the X-direction vibration displacement after the rotor is supported by the RAIAB increases with the increase of the rotation speed while the Z-direction vibration displacement remains basically unchanged.

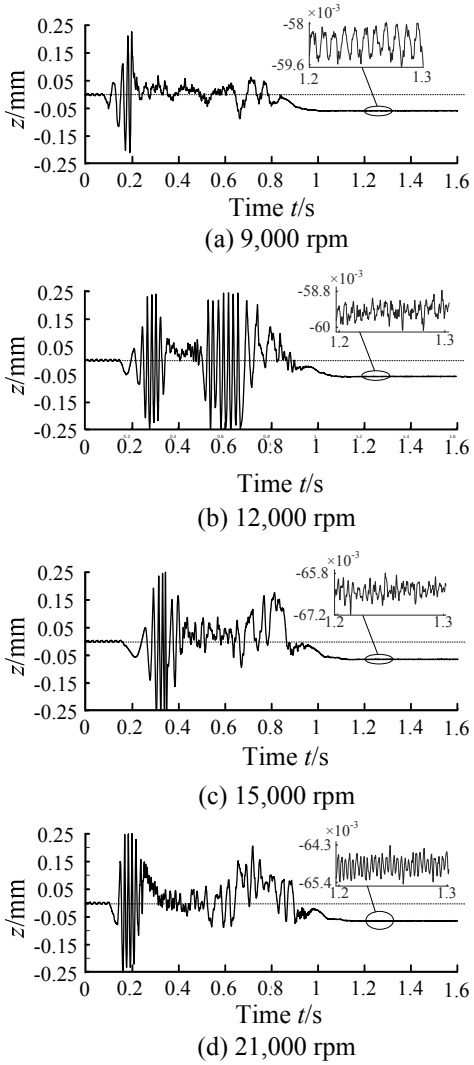

Figure 11. Displacement in the Z direction of the rotor at different rotational speeds

V. CONCLUSION

1. The axial clearance and actual clearance between the rotor and the inner bushing will be affected when the taper plan is adopted. When the rotor and the inner bushing are tapered with only one type of taper, the actual clearance will be smaller than the radial clearance ρ_r and it will be decreased with the increase of taper.

2. Compared to the rotor cone with only one kind of taper, the use of two taper combinations of the rotor cone can effectively reduce the generated axial force after the rotor falls.

3. The performance of RAIAB has been experimentally tested under the whole AMB fail conditions at different speeds. The test results show that the RAIAB can not only eliminate the radial protective clearance at both ends of the rotor, but also eliminate the axial displacement of the rotor in about 1 s. Then, the rotor could be stably supported at both radial and axial positions which are near its original center of each magnetic bearing.

4. In order to optimize the RAIAB, more factors should be considered later, such as the taper size of the rotor and the inner bushing, the clearance elimination time and so on. At the same time, more experimentally tests need to be explored to ensure the reliability of RAIAB.

REFERENCES

[1] Gerhard S, Maslen E H. Magnetic bearings theory, design, and application to rotating machinery [M]. *New York: Springer*, 2009: 1-26.

[2] YU L. Controllable magnetic suspension rotor system [M]. *Beijing: Science Press*, 2003: 1-7. (in Chinese)

[3] Xu L X, Zhou B. The current situation and development trend for more-electric gas turbine engines [J]. *Journal of Aerospace Power*, 2003, 18(1): 51-59. (in Chinese)

[4] Sun Z, Yan X, Zhao J, et al. Dynamic Behavior Analysis of Touchdown Process in Active Magnetic Bearing System Based on a Machine Learning Method[J]. *Science & Technology of Nuclear Installations*, 2017, 2017(5):1-11.

[5] Saket F Y, Sahinkaya M N, Keogh P S. Experimental assessment of touchdown bearing contact forces in magnetic bearing systems. *Proceedings of the 9th IFToMM International Conference on Rotor Dynamics*. *Springer,* 2015: 1501-1511.

[6] Ebrahimi R, Ghayour M, Khanlo H M. Chaotic Vibration Analysis of a Coaxial Rotor System in Active Magnetic Bearings and Contact With Auxiliary Bearings[J]. *Journal of Computational and Nonlinear Dynamics*, 2017, 12(3): 031012.

[7] Zeng S. Modelling and experimental study of the transient response of an active magnetic bearing rotor during rotor drop on back-up bearings [J]. *Proceedings of the Institution of Mechanical Engineers, Part I: Journal of Systems and Control Engineering*, 2003, 217(6): 505-517.

[8] Sun G. Rotor drop and following thermal growth simulations using detailed auxiliary bearing and damper models [J]. *Journal of Sound and Vibration*, 2006, 289(1): 334-359.

[9] Chen H M, Walton J, Heshmat H. Zero Clearance Auxiliary Bearings for Magnetic Bearing Systems [C]. *Orlando, Florida USA: ASME Turbo Expo' 97*, 1997.

[10] Salehi M, Heshmat H. On the Dynamic and Thermal Performance of a Zero Clearance Auxiliary Bearing (zcab) for a Magnetic Bearing System,' *Tribology Transaction*, 2000, 43(3): 435-440.

[11] Yu L, Geng H P, Qi S M, et al. Compliant Foil Bearings Used as Emergence Bearings [C]. *Proceedings of the Ninth International Symposium on Magnetic Bearings*, Lexington, Kentucky, USA, 2004: 129-136.

[12] Dellacorte C, Valco M J. Load Capacity Estimation of Foil Air Journal Bearings for Oil-Free Turbomachinery Applications [J]. *Tribology Transaction*, 2000, 43: 795-801.

[13] WU L S, Chen H, Shi T L, et al. Design of a new-style assistant bearing of magnetic bearing [J]. *Machinery Design and Manufacture*, 2010, 3: 32-34. (In Chinese)